Article

Au # N Synergy and N-Doping of Metal Oxide-Based Photocatalysts

Jesu#s Graciani, Akira Nambu, Jaime Evans, Jose# A. Rodriguez, and Javier Fdez. Sanz

J. Am. Chem. Soc., **2008**, 130 (36), 12056-12063 • DOI: 10.1021/ja802861u • Publication Date (Web): 14 August 2008

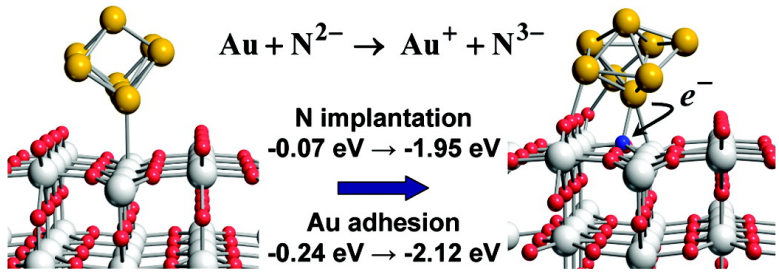

More About This Article

Additional resources and features associated with this article are available within the HTML version:

- Supporting Information
- Access to high resolution figures
- Links to articles and content related to this article
- Copyright permission to reproduce figures and/or text from this article

View the Full Text HTML

J|A|C|S
ARTICLES

Published on Web 08/14/2008

Au ↔ N Synergy and N-Doping of Metal Oxide-Based Photocatalysts

Jesús Graciani,[†] Akira Nambu,[‡] Jaime Evans,[§] José A. Rodriguez,[‡] and Javier Fdez. Sanz*,[†]

Departamento de Química Física, Facultad de Química, Universidad de Sevilla, E-41012, Sevilla, Spain, Chemistry Department, Brookhaven National Laboratory, Upton, New York, United States of America, and Facultad de Ciencias, Universidad Central de Venezuela, Caracas 1020 A, Venezuela

Received April 18, 2008; E-mail: sanz@us.es

Abstract: N-doping of titania makes photocatalytic activity possible for the splitting of water, and other reactions, under visible light. Here, we show from both theory and experiment that Au preadsorption on TiO_2 surfaces significantly increases the reachable amount of N implanted in the oxide. The stabilization of the embedded N is due to an electron transfer from the Au 6s levels toward the N 2p levels, which also increases the Au-surface adhesion energy. Theoretical calculations predict that Au can also stabilize embedded N in other metal oxides with photocatalytic activity, such as $SrTiO_3$ and ZnO, producing new states above the valence band or below the conduction band of the oxide. In experiments, the Au/TiN_xO_{2-y} system was found to be more active for the dissociation of water than TiO_2, Au/TiO_2, or TiO_{2-y}. Furthermore, the Au/TiN_xO_{2-y} surfaces were able to catalyze the production of hydrogen through the water-gas shift reaction (WGS) at elevated temperatures (575−625 K), displaying a catalytic activity superior to that of pure copper (the most active metal catalysts for the WGS) or Cu nanoparticles supported on ZnO.

I. Introduction

In industrial operations, H_2 is mainly produced by the steam-reforming of hydrocarbons, $C_nH_m + nH_2O \rightarrow nCO + (n + m/2)H_2$, and the water−gas shift reaction, $H_2O + CO \rightarrow H_2 + CO_2$. The well-known issues related to environmental and global warming concerns have generated a huge research effort in photoassisted reactions that make use of abundant, long lasting, and clean solar energy. Since the production of hydrogen through photoinduced water splitting on titania was discovered,[1] semiconductor-based photocatalysis has prompted many investigations, most of them focused on TiO_2. Beyond its high activity, the advantages of using TiO_2 as a photocatalyst include low cost, mechanical and thermal stability, environmental compatibility, and photocorrosion resistance. The main drawback of this material is related to its relatively large band gap, between 3.0−3.2 eV, which makes it useful only under ultraviolet (UV) light, or, in other words, only a small fraction (5%) of the solar spectrum is absorbed (λ < 380 nm).

In order to overcome this limitation, extending the absorption of TiO_2 into the wide visible light region seems to be a possible solution, and with this aim, doping of TiO_2 with both metal and non-metal impurities has been the subject of much research.[2−5] So far, one of the most promising materials that have been synthesized is N-doped TiO_2. Since the pioneering work of Asahi et al.,[6] nitrogen-doped TiO_2 has received a lot of attention[7] because the implantation of nitrogen modifies the electronic structure by introducing localized states to the top of the valence band, narrowing the band gap. This reduction of the band gap makes possible the photocatalytic activity in a number of reactions under visible light.[6,8−13]

The main drawback of N doping relies on the relatively low concentration (<2%) of dopant that can be implanted in titania.[14] Indeed, implanted N is unstable with respect to N_2 evolution.[15,16] Such an escape may be partially hindered by the presence of

[†] Departamento de Química Física, Facultad de Química, Universidad de Sevilla.
[‡] Chemistry Department, Brookhaven National Laboratory.
[§] Facultad de Ciencias, Universidad Central de Venezuela.

(1) Fujishima, A.; Honda, K. *Nature (London)* **1972**, *238*, 37.
(2) Hoffmann, M. R.; Martin, S. T.; Choi, W.; Bahnemannt, D. W. *Chem. Rev.* **1995**, *95*, 69–96.
(3) Choi, W.; Termin, A.; Hoffmann, M. R. *J. Phys. Chem.* **1994**, *98*, 13669–13679.
(4) Wang, Y.; Cheng, H.; Hao, Y.; Ma, J.; Li, W.; Cai, S. *Thin Solid Films* **1999**, *349*, 120–125.
(5) Anpo, M. *Catal. Surv. Jpn.* **1997**, *1*, 169–179.
(6) Asahi, R.; Morikawa, T.; Ohwaki, T.; Aoki, K.; Taga, Y. *Science* **2001**, *293*, 269–271.
(7) For a review of the N-doping process see the special issue: *Chem. Phys.* **2007**, 339.
(8) Chen, X.; Burda, C. *J. Phys. Chem. B* **2004**, *108*, 15446–15449.
(9) Torres, G. R.; Lindgren, T.; Lu, J.; Granqvist, C.-G.; Linquist, S.-E. *J. Phys. Chem. B* **2004**, *108*, 5995–6003.
(10) Nakamura, R.; Tanaka, T.; Nakato, Y. *J. Phys. Chem. B* **2004**, *108*, 10617–10620.
(11) Mrowetz, M.; Balcerski, W.; Colussi, A. J.; Hoffmann, M. R. *J. Phys. Chem. B* **2004**, *108*, 17269–17273.
(12) Sathish, M.; Viswanathan, B.; Viswanath, R. P.; Gopinath, C. S. *Chem. Mater.* **2005**, *17*, 6349–6353.
(13) Belver, C.; Bellod, R.; Stewart, S. J.; Requejo, F. G.; Fernández-García, M. *Appl. Catal., B* **2006**, *65*, 309–314.
(14) Batzill, M.; Morales, E.; Diebold, U. *Phys. Rev. Lett.* **2006**, *96*, 026103.
(15) Nambu, A.; Graciani, J.; Rodriguez, J. A.; Wu, Q.; Fujita, E.; Sanz, J. F. *J. Chem. Phys.* **2006**, *125*, 094706.
(16) Graciani, J.; Álvarez, L. J.; Rodriguez, J. A.; Sanz, J. F. *J. Phys. Chem. C* **2008**, *112*, 2624–2631.

10.1021/ja802861u CCC: $40.75

oxygen vacancies as a cooperative interaction between the dopant and the vacancy is established with further N stabilization through an electron transfer from the vacancy toward the partially occupied N 2p band.[16] The N stabilization via oxygen vacancies is obviously of limited utility. Thus, there is an active search for finding ways to enhance the amount of N which can be stabilized inside titania and other oxide semiconductors.

This synthetic problem could be overcome if one could stabilize implanted N by loading the surface with another species (a metal) able to donate electron density to the not fully occupied N 2p orbitals. We show in this work how Au ↔ N interactions lead to a stabilization of implanted N and how indeed it is possible to increase the N concentration of the surface by direct reaction of NH_3 with Au/TiO_2(110). On its turn, the presence of implanted N increases the interaction between the surface and the transition metal, whose charge increases. This synergic effect has an enormous potential both in heterogeneous catalysis and photocatalysis. Experimental tests for the new material, Au/TiN_xO_{2-y}, show it to be very active for the thermal dissociation of water and the water−gas shift (WGS) reaction at elevated temperatures (575−625 K).

II. Theoretical and Experimental Methods

II. a. Density-Functional Calculations. DFT calculations have been performed using the plane-wave-pseudopotential approach within the projector augmented wave method (PAW)[17] together with the GGA exchange correlation functional proposed by Perdew et al.[18] as implemented in the VASP 4.6 code.[19,20] A plane-wave cutoff energy of 400 eV was used. We considered the Ti (3*s*, 3*p*, 3*d*, 4*s*), Sr (4*s*, 4*p*, 5*s*), Zn (3*d*, 4*s, 4p*), O (2*s*, 2*p*), N (2*s*, 2*p*), and Au (5*d*, 6*s*) electrons as valence states, while the remaining electrons were kept frozen as core states. The Brillouin-zone integrations were performed using Monkhorst-Pack grids.[21] The calculations were carried out using a (8 × 8 × 10) mesh for TiO_2 rutile bulk (6 atoms), (6 × 6 × 4) for ZnO-wurzite bulk (4 atoms) and (6 × 6 × 6) for $SrTiO_3$ bulk (5 atoms). To obtain faster convergence with respect to the number of *k* points thermal smearing of one-electron states (k_BT = 0.05 eV) has been allowed using the Gaussian smearing method to define the partial occupancies. The calculated lattice parameters are in good agreement with experimental values (in parenthesis): 4.593 (4.594)[22] Å y 2.956 (2.958) Å for *a* and *c*, respectively, in the TiO_2 case, 3.278 (3.249)[23] Å and 5.301 (5.205) Å for *a* and *c*, respectively, in the ZnO case, and 3.942 (3.91)[24,25] Å in the SrTiO3 case.

We have used the most stable phase and surface for the three solids: rutile TiO_2 (110), wurzite ZnO (10$\bar{1}$0) and $SrTiO_3$ (001). Since the purpose of this work is to study the synergetic interaction between adsorbed gold and implanted nitrogen, the surface models should be able to represent adequately the experimental Au coverage and N concentration. We have chosen a (4 × 1) surface model for the adsorption of single gold atoms on TiO_2 (110), (4 × 2) for the adsorption of a gold cluster of 8 atoms, and (2 × 2) for the ZnO (10$\bar{1}$0) and $SrTiO_3$ (001) surfaces. With respect to the thickness of the slab models, care has to be taken with the rutile TiO_2 (110) surface due to the oscillating behavior observed in, for instance, surface energies and vacancies formations energies.[26] In order to avoid spurious effects due to the finite thickness of the slab, we used a recently published model of six layers[27,28] in which the two lowest layers are fixed at the optimized atomic bulk positions while the atoms in the upper four layers are allowed to relax. This model has been shown to minimize the well-known energy oscillations as a function of the number of layers (even−odd) and reaches convergence for both the geometric and electronic surface structures. We have chosen a model of fully relaxed 6 atomic-layers for represent the SrTiO3 (001) surface. We have used these two surface slab models successfully in previous works.[16,29] Finally, a model of fully relaxed 12 atomic-layers has been used for describe the ZnO (10$\bar{1}$0) surface.[30] For these surface models, the grids of *k*-points and the total amount of atoms were (2 × 4 × 1) for (4 × 1) TiO_2 (110) (144 atoms), (1 × 1 × 1) for (4 × 2) TiO_2 (110) (288 atoms), (4 × 4 × 1) for (2 × 2) $SrTiO_3$ (001) (60 atoms), and (4 × 2 × 1) for (2 × 2) ZnO (10$\bar{1}$0) (96 atoms).

II.b. Reaction of NH_3 with Au/TiO_2(110) and Water-Gas Shift Activity. The experiments described in section III were performed in an ultrahigh-vacuum (UHV) chamber that has attached a high-pressure cell or batch reactor.[31,32] The sample could be transferred between the reactor and vacuum chamber without exposure to air. The UHV chamber (base pressure ≈ 5 × 10^{-10} Torr) was equipped with instrumentation for X-ray photoelectron spectroscopy (XPS), low-energy electron diffraction (LEED), ion scattering spectroscopy (ISS), and thermal-desorption mass spectroscopy (TDS).

Au was vapor deposited on a TiO_2(110) following the methodology described in refs 31 and 33. Au was deposited on the oxide substrate at room temperature, and then the sample was heated to the elevated temperatures necessary for the implantation of nitrogen by exposure to NH_3 (770−780 K) or for the water−gas shift reaction (575−650 K). The WGS activity of the samples was investigated with a mixture of 20 Torr of CO and 10 Torr of H_2O.[33] The CO gas was cleaned of any metal carbonyl impurity by passing it through purification traps. In our reactor, a steady-state regime for the production of H_2 and CO_2 was reached after 2−3 min of reaction time. The kinetic experiments were done in the limit of low conversion (<5%). After each experiment with the Au/TiO_2 or Au/TiN_xO_{2-y} surfaces, the TiO_2(110) substrate was cleaned by Ar sputtering and annealing at elevated temperature.[15,33]

(17) Kresse, G.; Joubert, J. *Phys. Rev. B* **1999**, *59*, 1758.
(18) Perdew, J.; Chevary, J.; Vosko, S.; Jackson, K.; Pederson, M.; Singh, D.; Fiolhais, C. *Phys. Rev. B* **1992**, *46*, 6671.
(19) Kresse, G.; Hafner, J. *Phys. Rev. B* **1993**, *47*, 558–561.
(20) Kresse, G.; Furthmuller, J. *Comput. Mater. Sci.* **1996**, *6*, 15–50. Kresse, G.; Furthmuller, J. *Phys. Rev. B* **1996**, *54*, 11169–11186.
(21) Monkhorst, H. J.; Pack, J. D. *Phys. Rev. B* **1976**, *13*, 5188–5192.
(22) Burdett, J. K.; Hughbanks, T.; Miller, G. J.; Richardson, J. W.; Smith, J. V. *J. Am. Chem. Soc.* **1987**, *109*, 3639–3646.
(23) Sawada, H.; Wang, R.; Sleight, A. W. *J. Solid State Chem.* **1996**, *122*, 148–150.
(24) Wells, A. F. *Structural Inorganic Chemistry*; Oxford University Press: New York, 1987.
(25) Noguera, C. *Physics and Chemistry of Oxide Surfaces*; Cambridge University Press: Cambridge, 1996.
(26) Oviedo, J.; Sanz, J. F. *J. Chem. Phys.* **2004**, *121*, 7427–7433.
(27) Hameeuw, K. J.; Cantele, G.; Ninno, D.; Trani, F.; Iadonesi, G. *J. Chem. Phys.* **2006**, *124*, 024708.
(28) Thompson, S. J.; Lewis, S. P. *Phys. Rev. B* **2006**, *73*, 073403.
(29) Rodriguez, J. A.; Azad, S.; Wang, L.-Q.; Garcia, J.; Etxeberria, A.; Gonzalez, L. *J. Chem. Phys.* **2003**, *118*, 6562–6571.
(30) Cooke, D. J.; Marmier, A.; Parker, S. C. *J. Phys. Chem. B* **2006**, *110*, 7985–7991.
(31) Wang, X.; Rodriguez, J. A.; Hanson, J. C.; Pérez, M.; Evans, J. *J. Chem. Phys.* **2005**, *123*, 221101.
(32) Rodriguez, J. A.; Liu, P.; Hrbek, J.; Evans, J.; Perez, M. *Angew. Chem., Int. Ed.* **2007**, *46*, 1329.
(33) Rodriguez, J. A.; Liu, G.; Jirsak, T.; Hrbek, J.; Chang, Z.; Dvorak, J.; Maiti, A. *J. Am. Chem. Soc.* **2002**, *124*, 5242–5250.

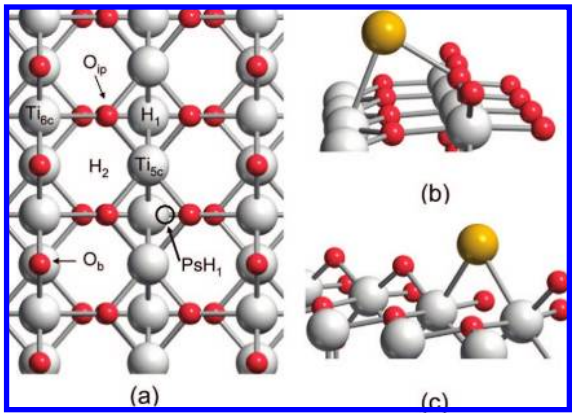

Figure 1. (a) Top view of the adsorption sites on the TiO_2(110) rutile surface. Geometries of the most stable structures for Au atom deposited on the stoichiometric (b) and reduced (c) TiO_2(110) rutile surface. Colors: Ti (soft-gray), O (soft-red), Au (yellow).

Table 1. Adsorption Energies (eV) of Au Atoms at Different Sites on the Stoichiometric (s), Reduced (r), and N Implanted TiO_2(110) Rutile Surface[a]

bonding atom	adsorption site	*s*-TiO_2	*r*-TiO_2	N-TiO_2
O	Ob	−0.29	−0.24	**−1.71**
	Oip	PsH1		
	Ti6c	−0.06	−0.08	−1.63
O−Ti	H_2	**−0.38**	−1.23	−1.68
	PsH1	−0.18	−1.24	−1.45
Ti	H_1	−0.13	−0.68	−1.31
	Ti5c	−0.27	−1.21	−1.18
N	N			PsH_1(N)
	PsH_1(N)			**−2.55**
Vacancy	V_b		**−1.55**	

[a] (See Figure 1 for labeling).

III. Results and Discussion

We start this section with the theoretical analysis of the interaction between gold atoms and TiO_2(110) surfaces at the different possible sites described in Figure 1. In agreement with previous work, we found that the interaction with the stoichiometric surface, *s*-TiO_2, is very low whatever the adsorption site is as shown in Table 1, the most stable state being a hollow position, H_2, in which Au binds a bridging oxygen, a 5-fold Ti center and two in-plane oxygen atoms (Figure 1b).[34−37] Also, both the density of states, DOS, and the Bader analysis show only a weak oxidation of gold ($q_{Au} = 0.07$ |e|). This is in contrast with what is found when Au atoms are deposited on a reduced surface, *r*-TiO_2. The metal−support interaction increases significantly when Au atoms lie at the Ti sites (or with nearby Ti centers). The most favored site is when the Au atoms are filling the bridge oxygen vacancies, V_b, (−1.55 eV, Figure 1c), also in agreement with previous calculations.[33,38,37,39−42] The analysis of the DOS now shows that the Au centers are partially reduced, with its 6s band almost completely filled up. This is also consistent with the estimated Bader charge of $q_{Au} = -0.42$ |e|. Such a reduction can be easily rationalized on the basis of the electron transfer from the partially reduced Ti 3d toward the half-filled Au 6s states. Indeed, when an oxygen defect is created, there are two extra electrons associated to the vacancy, which formally give place to two Ti^{3+} surface species. These electrons occupy the (higher energy) Ti 3d band and after Au deposition they move toward the lower energy Au 6s band.

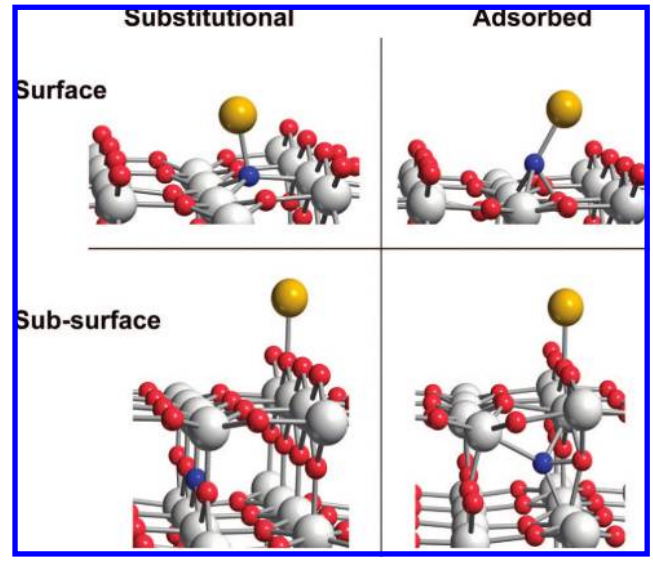

Figure 2. Optimized structures of Au atom deposited on N doped TiO_2(110) rutile surface. Colors: Ti (soft-gray), O (soft-red), N (blue), Au (yellow).

Table 2. Adsorption Energies (eV) and Bader Charges |e| for Au Atoms Deposited on Different N-Doped TiO_2(110) Rutile Surfaces

site		adsorption energy	direct contact	charge
substitut.	N_{ip}	−2.55	yes	0.33
	$N_b{}^2$	−1.71	no	0.55
adsorbed	PsH_1(N)	−2.12	yes	0.37
	interstitial	−0.79	no	0.51

Let us now consider the interaction between a gold atom and a nitrogen doped surface, N−TiO_2. Among the different possibilities of N adsorption/implantation on the TiO_2(110) surface,[16] we have selected the most stable and representative sites. These correspond to two purely substitutional positions belonging to either the surface and the subsurface, and two purely adsorbed N on either the surface or the subsurface (interstitial). As reported in ref 16, the most stable substitutional positions are the in-plane site, N_{ip}, for the first TiO_2 layer, and the bridge site, $N_b{}^2$, for the second layer. In the case of pure N adsorption, the on top of bridge oxygen, O_b, and the pseudohollow, PsH1, sites are degenerate and we have chosen the latter. On these structures, we have added a gold atom, and the optimized most stable structures are reported in Figure 2. The adsorption energies reported in Table 2 shows that the interaction is larger when there is direct bonding between Au and N atoms, which is only possible when N atom lies on the first layer of TiO_2 surface. The preferred site is found when Au

(34) Campbell, C. T.; Parker, S. C.; Starr, D. E. *Science* **2002**, *298*, 811–814.
(35) Vijay, A.; Millis, G.; Metiu, H. *J. Chem. Phys.* **2003**, *118*, 6536–6551.
(36) Pillay, D.; Hwang, G. S. *Phys. Rev. B* **2005**, *72*, 205422.
(37) Matthey, D.; Wang, J. G.; Wendt, S.; Matthiesen, J.; Schaub, R.; Laegsgaard, E.; Hammer, B.; Besenbacher, F. *Science* **2007**, *315*, 1692–1696.
(38) Lopez, N.; Norskov, J. K.; Janssens, T. V. W.; Carlsson, A.; Puig-Molina, A.; Clausen, B. S.; Grunwaldt, J.-D. *J. Catal.* **2004**, *225*, 86–94.
(39) Wahlström, E.; Lopez, N.; Schaub, R.; Thostrup, P.; Ronnau, A.; Africh, C.; Laegsgaard, E.; Norskov, J. K.; Besenbacher, F. *Phys. Rev. Lett.* **2003**, *90*, 026101.
(40) Remediakis, I. N.; Lopez, N.; Nørskov, J. K. *Angew. Chem., Int. Ed.* **2005**, *44*, 1824–1826.
(41) Laursen, S.; Linic, S. *Phys. Rev. Lett.* **2006**, *97*, 026101.
(42) Sanz, J. F.; Márquez, A. *J. Phys. Chem. C* **2007**, *111*, 3949.

Table 3. Adsorption Energies for Au (eV) and Implantation Energies for N (eV) in the Surfaces: TiO_2(110) Rutile, ZnO ($10\bar{1}0$) (both N-in and N-out sites are included) and $SrTiO_3$ (001) (SrO- and TiO- terminated)[a]

		TiO_2	TiO_2 (Au_8)	ZnO (N-out)	ZnO (N-in)	$SrTiO_3$ (SrO-)	$SrTiO_3$ (TiO-)
N	pure surface	−0.13	−0.07	−0.77	−1.01	−0.17	−0.45
implantation	preadsorbed Au	−2.50	−1.95	−2.51	−1.86	−1.80	−1.87
Au	pure surface	−0.18	−0.24	−1.00	−1.02	−1.18	−0.76
adsorption	preimplanted N	−2.55	−2.12	−2.74	−1.87	−2.81	−2.18
synergy (eV)		−2.37	−1.88	−1.74	−0.85	−1.63	−1.42

[a] In the case of TiO_2 we have included the data for the adsorption of a gold cluster of eight atoms. (See Figures 2, 5, 7, and 8 for labeling).

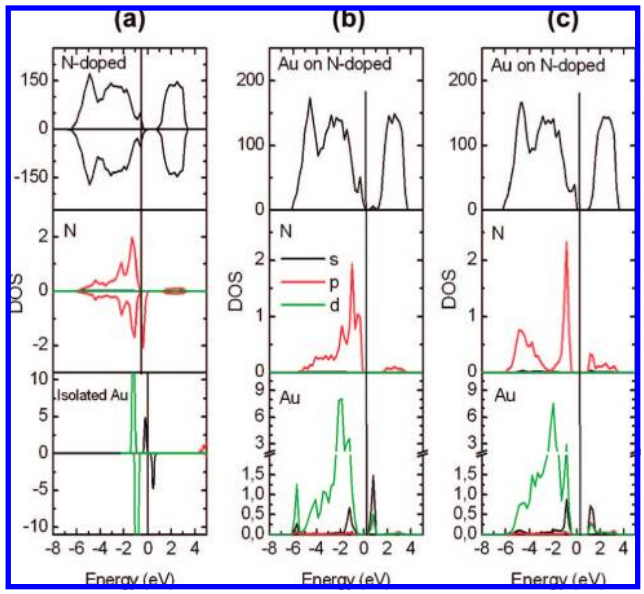

Figure 3. Density of states (DOS) plots for isolated Au(g) and N-TiO_2 (a). Au adsorbed on the N−TiO_2(110) surface, at two different sites: (b) H_2, and (c) PsH_1(N). The top panels show the total DOS, the middle panels the DOS projected on N atom and the bottom panels the DOS projected on Au atom. Vertical lines indicate the top of the valence band.

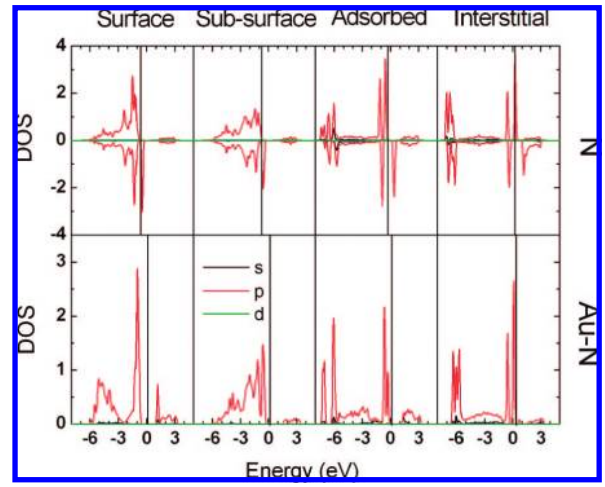

Figure 4. Nitrogen projected density of states (DOS) plots for the four structures depicted in Figure 2. The top panels correspond to the N−TiO_2(110) surface, while the bottom panels are obtained after Au deposition on the N−TiO_2(110) surface. Vertical lines indicate the top of the valence band.

atom is on top of N_{ip} with an adsorption energy of −2.55 eV. This preferred structure has been selected as the most representative one and has been further analyzed and compared with stoichiometric and reduced surfaces. As can be seen in Table 1, a significant increasing of the interaction energy with respect to both stoichiometric and reduced surfaces is observed. Such an increment is general and occurs both at the cationic and anionic sites of the surface. The analysis of the electronic structure shows that the simultaneous presence of both empty N 2p states in the low band gap region and the (higher energy) Au 6s partially filled band allows for an electron transfer between them. Indeed, the DOS plots reported in Figure 3 show that the electron density of Au (hybridized spd band) is pumped out and redirected toward the 2p orbitals of N atom which closes its shell. There is a noticeable energy gap between these orbitals which accounts for the large estimated interaction energy. Formally, the process might be written as $Au + N^{2-} \rightarrow N^{3-} + Au^{+}$, the estimated Bader charge now being $q_{Au} = 0.33$ |e|. However, it is also noteworthy that this electron transfer mechanism also occurs when N and Au are not in direct contact but they fall apart, as shown by the Bader charges reported in Table 2 that show a cationic behavior of Au whatever the site is. Notice, however, that the largest interaction energies (direct contact) are associated with the smallest positive charges clearly indicating that beyond this electron transfer mechanism of stabilization, a significant ionic contribution between the pair $Au^{+}-N^{3-}$, as well as covalent interactions are expected. Finally, to round up the electronic structure analysis, DOS plots for the four Au/N−TiO_2(110) cases have been reported in Figure 4. In the top panels the DOS projected on N atom shows that N 2p band is partially empty with outstanding beta features above the Fermi level. After doping with a gold atom, the N 2p band gets stabilized with clear shell closing (bottom panels).

However, besides the fact that the presence of implanted N atoms raises the interaction between Au atoms and the surface, one can wonder whether or not the presence of deposited Au atoms is also able to favor the process of N implantation on the surface. As we have recently shown, N implantation on the pristine TiO_2(110) surface at the in plane position is slightly exothermic (−0.12 eV). Yet, in the case that a gold atom is preadsorbed on the surface, the implantation process is exothermic by −2.50 eV. In other words, there is a synergism between implanted N and deposited Au atoms which leads to a higher stabilization of the former, and a stronger adsorption of Au atoms. Such a synergistic effect should not be limited to adsorbed single Au atoms, but should also occur with larger Au clusters. In fact, our calculations using a supported Au_8 cluster, see Figure 5, show a similar interaction energy (−2.12 eV), and again, the DOS analysis reveals that the N 2p band is filled up. Of course, the larger the interaction energy, the higher the diffusion barriers and, therefore, more difficult the sintering of particles. Nevertheless, this synergism suggests that preadsorbing gold atoms would allow for a more efficient N implantation on the surface which would provide either larger N concentrations, confirmed below through experiments of X-ray photoelectron spectroscopy (XPS), or less reconstructed surfaces.

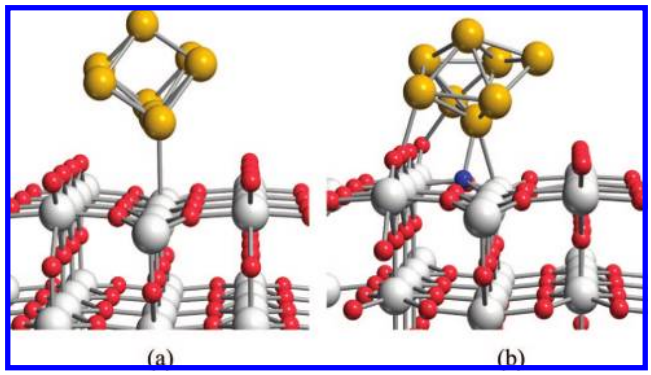

Figure 5. Geometries of the most stable structures for the adsorption of a cluster of eight Au atoms on the TiO_2(110) rutile surface: (a) pure and (b) N implanted surface. Colors: Ti (soft-gray), O (soft-red), N (blue), and Au (yellow).

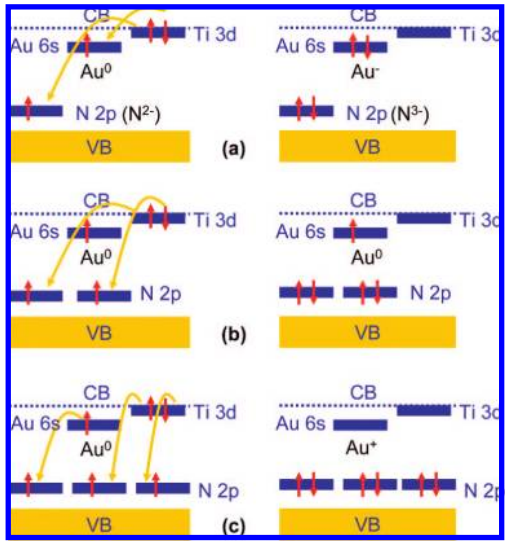

Figure 6. Schematic representation of the electron transfer processes that take place when Au is deposited on the TiO_2(110) rutile surface at different implanted nitrogen atoms/oxygen vacancies (N:V) ratios. N:V = 1:1 (a), 2:1 (b), and 3:1 (c). Left hand side draws describe the initial state and right side ones describe the final state. CB stands for the conduction band and VB for the valence band.

Before closing the theoretical part of this work, three more issues will be addressed. The first concerns the comparison of our data with those recently reported by Matthey et al. on the enhanced bonding of gold on oxidized TiO_2(110).[37] These authors reported a stronger adhesion of gold with an adsorption energy of −2.38 eV, in quite good agreement with our values of −2.12 (Au_8) and −2.55 (single Au atom) eV for the N implanted surface. In fact, the enhanced energy mechanism of gold-surface binding is quite similar to that here discussed for the N−TiO_2 surface, but now, the electron transfer takes place from the Au 6s orbitals toward the not completely full O 2p orbital resulting from the extra oxygen present in the oxidized surface.

The second issue refers to the well-known coexistence of oxygen vacancies and implanted N atoms on the TiO_2 surface,[14,15] as one can wonder how the gold-support interaction energy and bonding mechanism might be affected. To this aim, we have modeled this situation for different N implanted/oxygen vacancies ratios (N:V) schematized in Figure 6. For a 1:1 ratio (Figure 6a). the two electrons of the vacancy are transferred to the lower N 2p and Au 6s orbitals giving rise to a completely filled N and an anionic Au species (i.e., $Au^0 + N^{2-} + V^{2-} \rightarrow V^0 + N^{3-} + Au^{1-}$) and the metal−support interaction is expected to be similar to that on a reduced surface of TiO_2. For a N:V ratio of 2:1 (Figure 6b), the two electrons of the vacancy may be accommodated in the two N 2p holes, the Au atom remaining almost unaltered (i.e., $Au^0 + 2N^{2-} + V^{2-} \rightarrow V^0 + 2N^{3-} + Au^0$), and the metal-surface interaction is expected to be similar to that of gold atoms deposited on a stoichiometric oxide surface. Finally, for a N:V ratio of 3:1 (or higher), Figure 6c, the two electrons of the oxygen vacancy will fill two of the N 2p holes and still will be enough room to accommodate one Au 6s electron, and therefore cationic-like gold species are expected. Thus, the N:V ratio tunes the metal-surface interaction energy and the charge of the gold deposited on the surface.

In addition to the analysis of the effect that the presence of vacancies induces on the adsorption of Au atoms, we can examine how the simultaneous presence of Au and implanted N affects the energy of formation of bridge oxygen vacancies. As reported in ref 16, the energy needed to create a vacancy diminishes from 3.29 (pristine surface) to 1.49 eV (N-doped surface). This stabilization is again due to the electron shift from the Ti 3d vacancy states toward the N 2p orbitals. On its turn, as stated above, Au atoms adsorb stronger on reduced surfaces, which can also be seen as a stabilization of the vacancy itself. Actually, the vacancy formation energy when an Au atom is adsorbed on the surface is of 2.02 eV. Compared to the N-doped surface, the lowering is smaller as now the electrons move from the Ti 3d band to the Au 6s orbital whose energy is higher than the N 2p levels. When there are both Au and N on the surface, removing a bridge oxygen adjacent to an Au−N pair involves an energy of 3.1 eV, only slightly lower to the undefective surface (3.29 eV). However, this is not the most favored state but Au atom is stabilized when moves and fills the vacancy. This state corresponds to a vacancy formation energy of 2.45 eV. In summary, taking as reference the energy of vacancy formation of a N-doped TiO_2(110) surface, we find that the presence of gold on the surface hampers the creation of oxygen vacancies. This result also applies when the concentration of implanted N is larger. For instance, to create a vacancy when there are two N atoms by supercell costs only 0.13 eV. However, if one Au atom is added to the surface, then the energy to create a vacancy jumps to 1.59 eV. Notice that adding two N atoms by supercell leads in the present case to a nonrealistic high concentration of surface N (12.5%), and therefore, it has to be considered just as a model for discussion.

The final issue to be analyzed with DF calculations refers to the implantation of N in other oxide semiconductors used in photocatalysis, namely $SrTiO_3$ and ZnO. There is also an interest in doping these oxides with N.[43] Using a six-layer slab for modeling the $SrTiO_3$(001) system,[29] see Figure 7, we found that the presence of Au, indeed, facilitates the implantation of N in the SrO- and TiO-terminated faces (Table 3). The energy released for the implantation of N on the SrO-terminated surface is only −0.17 eV, but increases to −1.80 eV when Au is present. Simultaneously, the adsorption energy of Au goes from −1.18 eV (no N) to −2.81 eV (N embedded). For the implantation of N on the TiO-terminated surface, the release of energy for the implantation of N is −0.45 eV without Au present and −1.87 eV with Au present. On this surface, the adsorption energy of Au is −0.76 eV for the stoichiometric system and −2.18 eV

(43) Wang, J.; Yin, S.; Komatsu, M.; Zhang, Q.; Saito, F.; Sato, T. *Appl. Catal. B: Environ.* **2004**, *52*, 11–21.

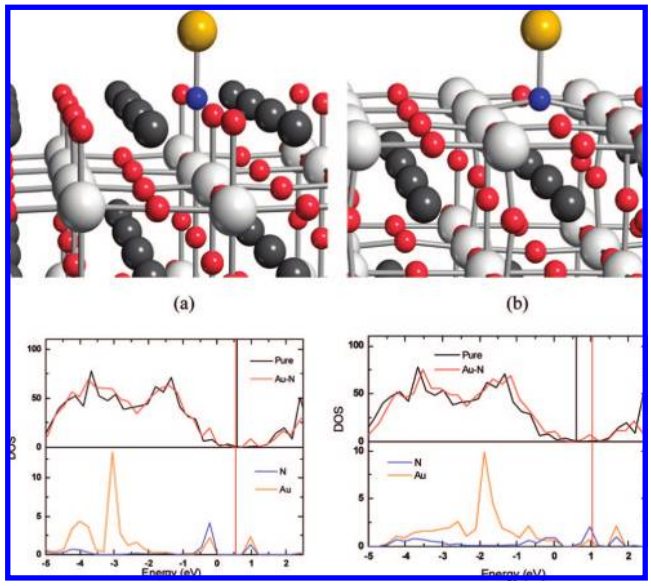

Figure 7. (Top) Geometries of the most stable structures for the adsorption of Au atoms on the N-implanted $SrTiO_3$ (001) surface: (a) SrO- and (b) TiO- terminated surfaces. Colors: Ti (soft-gray), Sr (dark-gray), O (soft-red), N (blue), and Au (yellow). (Bottom) Total DOS plots for the pure and for the N-implanted Au-loaded surfaces (top panels) and DOS projected on Au and N atoms in the N-implanted Au-loaded system (bottom panels). Vertical lines show the Fermi level in each case.

for the system with N implanted. Thus, as in the case of Au/TiN_xO_{2-x}(110), there are clear synergy effects for the coadsorption of Au and N on $SrTiO_3$(001), see Table 3. In the case of ZnO (Figure 8), the Au adsorption energy increases from −1.0 (clean surface) to −2.74 eV (N doped). Concomitantly, the N implantation energy drops from −2.51 (Au preadsorbed) to −0.77 eV (perfect surface). Moreover, this synergistic effect could be important in the photocatalytic processes under visible light on these surfaces since the Au ↔ N interactions in the surface led to the appearance of new levels just above the valence band and below the conduction band of $SrTiO_3$ (Figure 7) and ZnO (Figure 8). These extra levels should play a key role in the photodissociation of water.

In order to corroborate the theoretical predictions for Au/TiN_xO_{2-y}, we have carried out a series of experimental tests. Two types of TiO_2 systems were used: the surface (110) of a rutile single crystal and a polycrystalline film. The TiO_2 systems were prepared and cleaned in an ultrahigh vacuum (UHV) chamber that has capabilities for surface characterization and a small batch reactor attached.[33,44] In the batch reactor, the clean TiO_2(110) and TiO_2 surfaces were exposed to a mixture of 5 Torr of NH_3 and 95 Torr of He at 500 C for a period of 15 min. Then, the gases were pumped out and N 1s XPS spectra taken in the UHV chamber showed that there was not incorporation of N into the oxide lattice. In a second set of experiments, we vapor deposited different coverages of Au (up to 3 monolayers, ML) on the titania substrates following a previously described methodology.[33] Au is known to grow on titania forming three-dimensional particles.[45] The Au/TiO_2(110) and Au/TiO_2 surfaces were exposed to a mixture of 5 Torr of

(44) The sample could be transferred between the reactor and UHV chamber without exposure to air. The UHV chamber (base pressure ~ 1 × 10−10 Torr) was equipped with instrumentation for XPS, low-energy electron diffraction, ion-scattering spectroscopy, and thermal-desorption mass spectroscopy.

(45) Valden, M.; Lai, X.; Goodman, D. W. *Science* **1998**, *281*, 1647–1650.

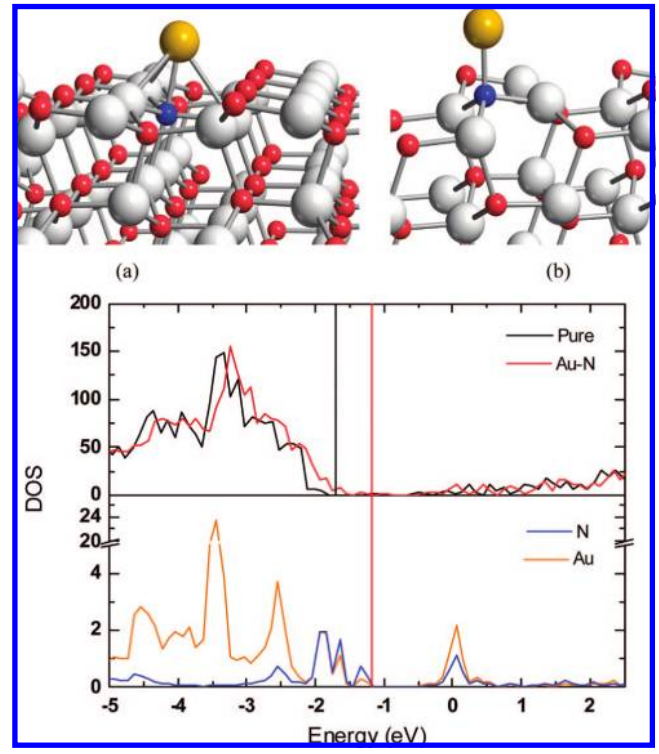

Figure 8. (Top) Geometries of the most stable structures for the adsorption of Au atoms on the N-implanted ZnO ($10\bar{1}0$) surface: N-implanted (a) in the second outermost (N-in) and (b) in the outermost (N-out) layer. Colors: Zn (soft-gray), O (soft-red), N (blue), Au (yellow). (Bottom) Total DOS plots for the pure and for the N-implanted Au-loaded surface (top panel) and DOS projected on Au and N atoms (bottom panels) for the most stable case (N-out). Vertical lines show the Fermi level in each case.

NH_3 and 95 Torr of He at 500 C for a period of 15 min. Subsequent XPS spectra indicated the incorporation of N into the oxide matrix, in agreement with the predictions of the theoretical calculations discussed above. Typical XPS results are shown in Figure 9. The TiO_2 film precovered with 0.5 ML of Au and exposed to NH_3 at elevated temperature exhibits two overlapping peaks in the N 1s region. The peak near 395.5 eV can be attributed to the formation of TiN, while the peak at ~397.2 eV could be due to N incorporated into TiO_2.[15] In the case of the TiO_2(110) surface precovered with 0.5 ML of Au, only the peak at ~397.2 eV is seen and the amount of N incorporated into the single crystal substrate is much smaller than in the case of the TiO_2 film. In the corresponding Ti 2p XPS spectrum there was a very small amount of Ti^{3+} in the TiO_2(110) single crystal after the implantation of N. This is again in very good agreement with the theory which predicts no formation of vacancies if gold is present. Significant amounts of Ti^{3+} and $Ti^{\delta+}$ (δa < 3) were found in the titania film after implantation of N, consistent with the formation of TiN in this system. Upon the incorporation of nitrogen, there were not big changes in the line-shape or peak positions of the Au 4f spectra, suggesting that no Au_xN species were formed.[31] The photoemission data are consistent with a configuration in which N is embedded in the titania lattice and interacting with the adsorbed Au.

Figure 10 shows the effects of Au coverage on the uptake of N in TiO_2(110) and TiO_2 surfaces. In test experiments, it was found that the implantation of N reached saturation after 5−10 min of exposure to NH_3. However, the data in the Figure 10 were all acquired after a NH_3 exposure of 15 min to ensure

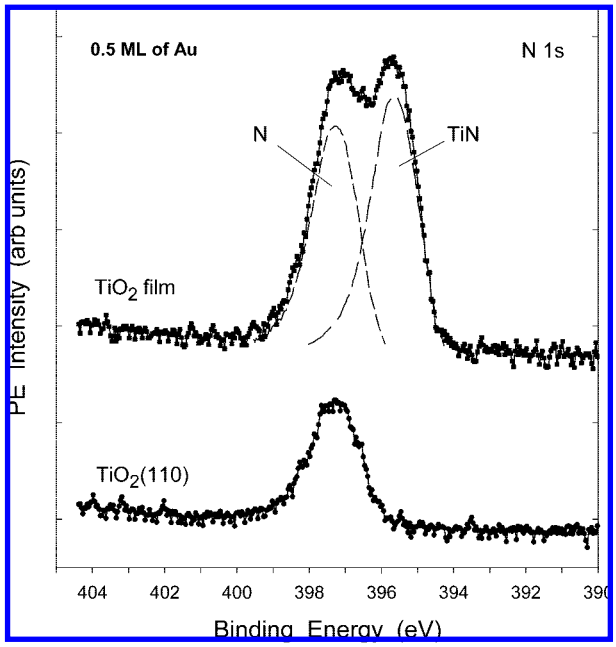

Figure 9. N 1s XPS spectra collected after exposing a $TiO_2(110)$ surface and a TiO_2 film, precovered with 0.5 ML of Au, to a mixture of 5 Torr of NH_3 and 95 Torr of He at 500 C for a period of 15 min.

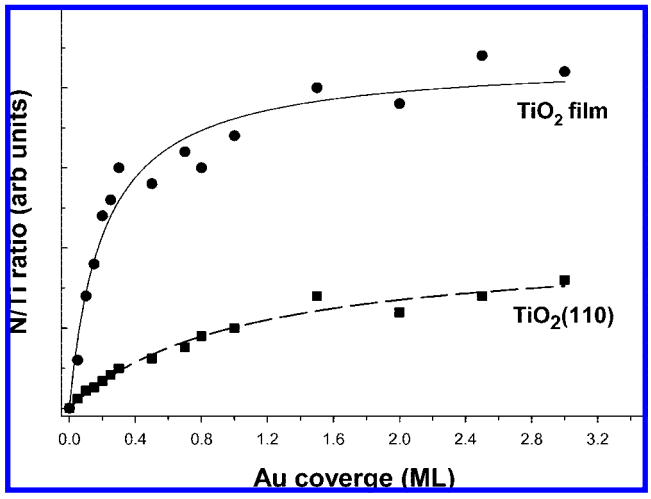

Figure 10. Effect of Au coverage on the amount of N incorporated after exposing a $TiO_2(110)$ surface and a TiO_2 film to a mixture of 5 Torr of NH_3 and 95 Torr of He at 500 C for a period of 15 min. The uptake of N was assumed to be proportional to the N1s to Ti 2p intensity ratio in XPS.

saturation. The N/Ti ratio was estimated from the relative areas of the N 1s and Ti 2p features in XPS. If there is not Au on the surface, there is not implantation of N at all at the investigated conditions. Surprisingly, in the presence of preadsorbed Au, the amount of implanted N becomes as high as 6% in the single crystal surface and ~20% in the polycrystalline film. The higher amount of implanted N in the film is attributable to the higher concentration of defects in a polycrystalline system. In a previous work, we have shown that vacancies and other lattice defects should be preferential sites for N adsorption/incorporation.[16] In Figure 10, the amount of incorporated N increases rapidly up to Au coverages of 0.4−0.5 ML. It is likely that only small Au nanoparticles are efficient for the dissociation of NH_3 and the production of the N atoms that will be incorporated into the titania lattice. When the gold coverage is above 1.5

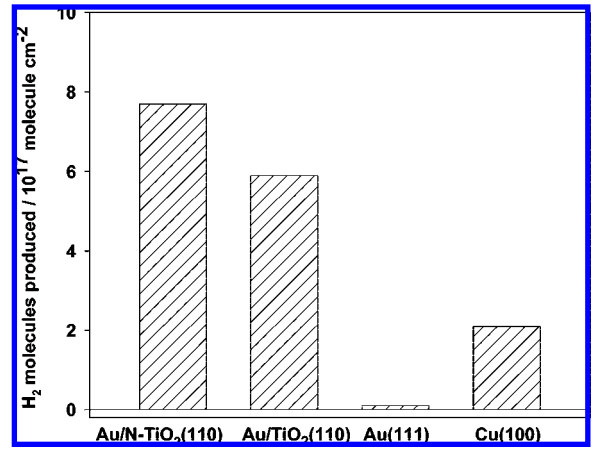

Figure 11. Water−gas shift activity of Cu(100), Au(111), and 0.5 ML of Au supported on clean $TiO_2(110)$ or on an oxide substrate with 5% N. The reported values for the production of H_2 were obtained after exposing the catalysts to 20 Torr of CO and 10 Torr of H_2O at 625 K for 5 min. The number of H_2 molecules produced is normalized by the surface area.[31]

ML, the metal particle size is expected to be large (>5 nm),[45] and the uptake of N is very small. For the systems in Figure 10, the binding energy of the Au 4f core levels decreased (0.1−0.4 eV) as the Au coverage increased. A simple interpretation can be argued: at small Au coverage, most of the Au atoms are involved in the Au ↔ N charge transfer seen in the DF calculations and the Au core levels appear at high binding energy. When the Au coverage increases, the Au atoms that are not bonded to N reduce the core level binding energy and bring it to a position close to that of pure metallic Au.

Experiments of high-resolution photoemission were done at beamline U7A[15,33] of the National Synchrotron Light Source to study the interaction between Au and N-doped $TiO_2(110)$. N was implanted into the oxide by ion sputtering using N_2 as a precursor.[15] The deposition of Au on the N-doped $TiO_2(110)$ at room temperature induced a decrease of 0.2−0.4 eV in the N 1s binding and no significant shifts in the Ti 2p binding energy. The high-resolution photoemission results point to a direct interaction of gold with nitrogen and are consistent with a Au ↔ N charge transfer.

The relatively large concentration of N in Au/TiN_xO_{2-y} makes this system attractive for the $H_2O \rightarrow H_2$ conversion in heterogeneous catalysis and photocatalysis (see Introduction). The interaction of H_2O with rutile $TiO_2(110)$ has been extensively investigated.[46] In general, previous studies have shown that O vacancies in the surface of $TiO_2(110)$ are necessary for the thermal dissociation of water. Our experiments for the dissociation of water on $Au/TiN_xO_{2-y}(110)$ at temperatures ranging from 300 to 650 K show systems that are more efficient for O−H bond cleavage than $TiO_2(110)$, $Au/TiO_2(110)$ or $TiO_{2-x}(110)$. Thus, while $TiO_2(110)$ is inactive as a catalysts for the water−gas shift reaction, Au/TiN_xO_{2-y} displays a high activity. Figure 11 shows the WGS activity of a $Au/TiN_xO_{2-y}(110)$ surface which contains 0.5 ML of Au and ~5% of N implanted in the titania lattice. Cu(100), one of the most active metal surfaces in the water−gas shift, is ~4× less active than the Au/TiN_xO_{2-y} (110) surface. This surface also has a higher WGS activity than Cu nanoparticles supported on ZnO.[32] Furthermore, the synergy between Au and N produces a system that is more catalytically active than $TiO_2(110)$, Au(111), or $Au/TiO_2(110)$.

(46) Henderson, M. A. *Surf. Sci. Rep.* **2002**, *46*, 5–308.

Postreaction surface analysis with XPS indicated that almost no N was removed from the $Au/TiN_xO_{2-y}(110)$ system during the water−gas shift process, but 30−40% of the initial N was transformed into NO_3.

IV. Summary and Conclusions

Nitrogen-doped metal oxides are promising materials for the production of hydrogen through the photocatalytic splitting of water although its applicability seems to be seriously hindered by the low N concentration that can be reached. We have shown theoretically and experimentally that Au adsorption on N-doped TiO_2 surfaces significantly stabilizes the implanted N, thus increasing the N loading reachable. Such stabilization is due to an electron transfer from the Au 6s levels toward the 2p levels of implanted N, filling up its electronic shell. An outstanding consequence of this new method for N-doping is that by controlling the N:V ratio, we could control the strength (and in some way the nature) of the metal-support interaction and the oxidation state of the supported gold atoms in contact with the surface, which could influence the growing mode of the gold nanoparticles, as well as their dispersion and resistance to sintering. Moreover, the Au/TiN_xO_{2-y} system was found to be active for the thermal dissociation of water and the production of H_2 through the water−gas shift reaction. Au ↔ N interactions also stabilize the implantation of N in the SrO- and TiO-terminated surfaces of $SrTiO_3$ or in ZnO. Coadsorption with Au appears therefore as an attractive approach for facilitating the embedding of N in oxide photocatalysts and for enhancing the adhesion of Au clusters on the surface.

Acknowledgment. This work was funded by the Ministerio de Educación y Ciencia, MEC, from Spain (project MAT2005-01872), and the Junta de Andalucía (project FQM-132). J.G. also gratefully acknowledges the MEC for a predoctoral grant. We also thank the computational resources provided by the Barcelona Supercomputing Center—Centro Nacional de Supercomputación (Spain). The work done at Brookhaven National Laboratory was supported by the U.S. Department of Energy, Division of Chemical Sciences (DE-AC02-98CH10886). J.E. thanks INTEVEP for a travel grant that made possible a part of this project. J.G. and J.F.S. thanks Prof. M.A. Álvarez for her continuous and enthusiastic support.

JA802861U